



## Measurement of the Top Quark Mass in the Lepton+Jets Channel Using the Matrix Element Method on $3.6 \text{ fb}^{-1}$ of DØ Run II Data

The DØ Collaboration  
URL <http://www-d0.fnal.gov>  
(Dated: 9th March 2009)

A measurement of the top quark mass in the lepton+jets channel of top quark pair production using the matrix element method is presented. The measurement is performed on a data sample of about  $3.6 \text{ fb}^{-1}$  of integrated luminosity acquired by the DØ experiment in Run II of the Fermilab Tevatron Collider at a center-of-mass energy  $\sqrt{s} = 1.96 \text{ TeV}$ . The purity of the data sample is enhanced by the application of a neural net-based  $b$ -tagging technique. In addition to the top quark mass, an overall multiplicative scale factor for jet energy calibration is included in the fit to data. This scale factor is constrained by the mass of hadronically decaying  $W$  bosons in top quark pair production, and by the independent jet energy scale from the calibration derived using photon+jets and dijet samples. The combination of the  $e$ +jets and  $\mu$ +jets channels for the  $b$ -tagged analysis on  $2.6 \text{ fb}^{-1}$  of Run IIb data yields

$$m_{\text{top}} = 174.8 \pm 1.3(\text{stat} + \text{JES}) \pm 1.4(\text{syst}) \text{ GeV}.$$

Combining this result with the  $b$ -tagged analysis on  $1.0 \text{ fb}^{-1}$  of Run IIa data yields

$$m_{\text{top}}(3.6 \text{ fb}^{-1}) = 173.7 \pm 0.8(\text{stat}) \pm 1.6(\text{syst}) = 173.7 \pm 1.8 \text{ GeV}.$$

## I. INTRODUCTION

The top quark was discovered [1, 2] in 1995 by the CDF and DØ experiments at the Fermilab Tevatron proton-antiproton Collider. The mass of the top quark, which is by far the heaviest of all quarks, plays an important role in electroweak radiative corrections and therefore in constraining the mass of the Higgs boson. Precise measurements of the top quark mass provide a crucial test of the consistency of the Standard Model (SM) and could indicate a hint of physics beyond the SM.

The Tevatron is still the only place where top quarks can be produced and studied directly. At the Tevatron, top quarks are mostly produced in pairs via the strong interaction. In the framework of the SM, the top quark decays to a  $W$  boson and  $b$  quark nearly 100% of the time. Events from top quark pair production are classified according to  $W$  boson decay channels. An event is referred to as “dilepton” if both  $W$  bosons decay leptonically to an electron or a muon and the corresponding neutrino, “all jets” if both  $W$  bosons decay hadronically, and “lepton+jets” if one of the  $W$  bosons decays leptonically and the other one hadronically. (Tau leptons are not explicitly reconstructed in this analysis.) Among these channels, the lepton+jets channel is particularly well suited for studies of top quark properties. It has not only a sizable branching fraction ( $\approx 38\%$ ) but also a striking signature, including an isolated lepton with large  $p_T$ , large missing transverse energy  $\cancel{E}_T$  from the undetected neutrino, and four or more jets with large transverse momentum, two of which originate from the hadronization of a  $b$  quark.

In this note, we present a measurement of the top quark mass in the lepton+jets channel of top quark pair production. Previous measurements of the top quark mass in the lepton+jets channel are described in [3–7]. The current measurement uses the matrix element method described in [4, 6, 7]. This method, which was pioneered and first successfully applied in [3], has consistently yielded high precision results. The data used for the current measurement were collected by the upgraded DØ detector [8] in Run II of the Tevatron at a center-of-mass energy  $\sqrt{s} = 1.96$  TeV, corresponding to about  $3.6 \text{ fb}^{-1}$  of integrated luminosity acquired from April 2002 until February 2006 (Run IIa) and from June 2006 until September 2008 (Run IIb). The data analysis on the  $1.0 \text{ fb}^{-1}$  of Run IIa data has been described in great detail in [6]. In this note, we describe the analysis on the Run IIb data of about  $2.6 \text{ fb}^{-1}$  of integrated luminosity. We then present the top quark mass obtained by combining the separate Run IIa and Run IIb results. In the following, unless otherwise noted, it is the Run IIb analysis that is described.

## II. EVENT SELECTION

The event selection is designed to define a data sample enriched in top quark pair events. An event is required to fire at least one of the DØ single lepton or lepton+jets triggers. The event vertex must be within 60 cm of the center of the detector along the beam direction, and must have at least three tracks attached to it. The event is required to contain one isolated lepton with  $p_T > 20$  GeV and a pseudo-rapidity  $|\eta| < 1.1$  ( $|\eta| < 2$ ) for electrons (muons). It is also required to have exactly four jets with  $p_T > 20$  GeV and  $|\eta| < 2.5$ , at least one of them with  $p_T > 40$  GeV. The missing transverse energy  $\cancel{E}_T$  is required to be larger than 20 (25) GeV in the  $e$ +jets ( $\mu$ +jets) channel. A cut on the azimuthal angle between  $\cancel{E}_T$  and the lepton momentum is imposed to exclude events where the transverse energy imbalance is caused by a poor measurement of the lepton energy. Events in which there is a second lepton are explicitly vetoed in order to ensure that the  $e$ +jets and  $\mu$ +jets channels are orthogonal to each other and to the dilepton analysis.

The dominant background contribution in the lepton+jets channel is  $W$  boson production with associated jets ( $W$ +jets). The second dominant background contribution is multijet production in which a jet is misidentified as a lepton. By identifying the  $b$  jets in the final state, these background contributions can be substantially reduced. A neural network (NN)  $b$ -tagging tool has been developed for this purpose. It takes advantage of the fact that the  $B$  hadrons can travel several millimeters before decaying due to their relatively long lifetime. The NN has been trained on QCD  $b\bar{b}$  and light-jet Monte Carlo (MC) samples, and its performance has been measured from data. In this analysis an event is required to have at least one  $b$ -tagged jet. This requirement retains about 70% of top quark pair events and increases the fraction of top quark pair events in the sample by a factor of two from about 35% to about 70%. There are 312 (303) events selected in the  $e$ +jets ( $\mu$ +jets) channel.

## III. THE MATRIX ELEMENT METHOD

To maximize the statistical information on the top quark mass extracted from the event sample, a probability is calculated for each event as a function of the assumed top quark mass  $m_{\text{top}}$  and an overall multiplicative jet energy scale factor  $JES$ . The factor  $JES$  is fitted in situ in data simultaneously with the top quark mass by using information from the invariant mass of the hadronically decaying  $W$  bosons. For every event, this mass is constrained to be equal

to the known value of the  $W$  boson mass. The probabilities from all events in the sample are then combined to obtain the sample probability as a function of  $m_{\text{top}}$  and  $JES$ , and the top quark mass is extracted by finding the values that maximize this probability. The probability  $P_{\text{evt}}$  for one event is composed from probabilities for two processes, top quark pair production and  $W$ +jets production, as

$$P_{\text{evt}}(x; m_{\text{top}}, JES, f_{\text{top}}) = f_{\text{top}} \cdot P_{\text{sig}}(x; m_{\text{top}}, JES) + (1 - f_{\text{top}}) \cdot P_{\text{bkg}}(x; JES). \quad (1)$$

Here,  $x$  denotes the kinematic variables of the event (jet and lepton energies and angles),  $f_{\text{top}}$  the signal fraction of the event sample, and  $P_{\text{sig}}$  and  $P_{\text{bkg}}$  the probability densities for observing  $x$  given a top quark pair and  $W$ +jets production event, respectively. Multijet background shape is assumed to be similar to that of  $W$ +jets and is not included in the background calculation. The effect of the difference in shapes between multijet and  $W$ +jets is accounted for in the systematic uncertainty.

The differential probability to observe a top quark pair event with object kinematics  $x$  in the detector is given by

$$P_{\text{sig}}(x; m_{\text{top}}, JES) = \frac{1}{\sigma_{\text{obs}}(p\bar{p} \rightarrow t\bar{t}; m_{\text{top}}, JES)} \times \sum_{\text{perm}} w_n \int_{q_1, q_2, y} \sum_{\text{flavors}} dq_1 dq_2 f(q_1) f(q_2) \frac{(2\pi)^4 |\mathcal{M}(q\bar{q} \rightarrow t\bar{t} \rightarrow y)|^2}{2q_1 q_2 s} d\Phi_6 W(x, y; JES). \quad (2)$$

Here, the symbol  $\mathcal{M}$  denotes the matrix element for the process  $q\bar{q} \rightarrow t\bar{t} \rightarrow b(l\nu)b(qq)$ ,  $s$  the  $p\bar{p}$  center-of-mass energy squared,  $q_1$  and  $q_2$  the momentum fractions of the colliding partons (which are assumed to be massless) within the colliding proton and antiproton,  $d\Phi_6$  an element of six-body phase space, and  $f(q)$  the probability density to find a parton of given flavor and momentum fraction  $q$  in the proton or antiproton. The finite detector resolution is taken into account via a convolution with a transfer function  $W(x, y; JES)$  that describes the probability to reconstruct a partonic final state  $y$  as  $x$  in the detector. Since it is not known from which parton a jet originates, a sum must be made over all 24 permutations of jet-to-parton assignments. Here  $w_n$  represents the weight of each permutation:

$$w_n = w_{J_i}(q_1) w_{J_j}(q_2) w_{J_k}(q_3) w_{J_l}(q_4) \quad (3)$$

where the weight for a  $b$ -tagged jet  $w_{\text{jet}}(q)$  is the  $b$ -tagging efficiency  $\epsilon(q; p_T, \eta)$  for a jet of transverse momentum  $p_T$  and pseudo-rapidity  $\eta$  originating from a parton of flavor  $q$  ( $=b, c$ , light quark or gluon). The weight for an un-tagged jet, on the other hand, is given by  $1 - \epsilon(q; p_T, \eta)$ .

The transfer function  $W(x, y; JES)$  factorizes into contributions from the individual top pair decay products. The angles of these decay products are assumed to be well-measured, while their energy or transverse momentum resolutions are determined from MC simulations. Here we describe as an example the jet energy transfer function  $W_{\text{jet}}(E_x, E_y; JES)$  which tells the probability for a measured jet energy  $E_x$  if the true quark energy is  $E_y$ . For the case  $JES = 1$ , the jet energy transfer function is parameterized as

$$W_{\text{jet}}(E_x, E_y; JES = 1) = \frac{1}{\sqrt{2\pi}(p_2 + p_3 p_5)} \left[ \exp\left(-\frac{((E_x - E_y) - p_1)^2}{2p_2^2}\right) + p_3 \exp\left(-\frac{((E_x - E_y) - p_4)^2}{2p_5^2}\right) \right]. \quad (4)$$

The  $p_i$  are linear functions of the quark energy, whose parameters are determined from fully simulated MC events. A different set of parameters is derived for each of four pseudo-rapidity  $\eta$  regions:  $|\eta| < 0.5$ ,  $0.5 < |\eta| < 1.0$ ,  $1.0 < |\eta| < 1.5$ , and  $1.5 < |\eta| < 2.5$ , and for three different quark varieties: light quarks ( $u, d, s, c$ ),  $b$  quarks with a soft muon tag in the associated jet, and all other  $b$  quarks. The derived jet energy transfer functions for light quarks are shown in figures 1. For  $JES \neq 1$ , the jet transfer function is adapted as follows:

$$W_{\text{jet}}(E_x, E_y; JES) = \frac{W_{\text{jet}}\left(\frac{E_x}{JES}, E_y; 1\right)}{JES}. \quad (5)$$

The  $JES$  factor is needed in the denominator to preserve the normalization  $\int W_{\text{jet}}(E_x, E_y; JES) dE_x = 1$ .

The corresponding overall detector efficiency depends both on  $m_{\text{top}}$  and on  $JES$ . This is taken into account in the cross section of top quark pair production observed in the detector:

$$\sigma_{\text{obs}}(p\bar{p} \rightarrow t\bar{t}; m_{\text{top}}, JES) = \int_{q_1, q_2, x, y} d\sigma(p\bar{p} \rightarrow t\bar{t} \rightarrow y; m_{\text{top}}) W(x, y; JES) f_{\text{acc}}(x), \quad (6)$$

where  $f_{\text{acc}}$  denotes the detector acceptance.

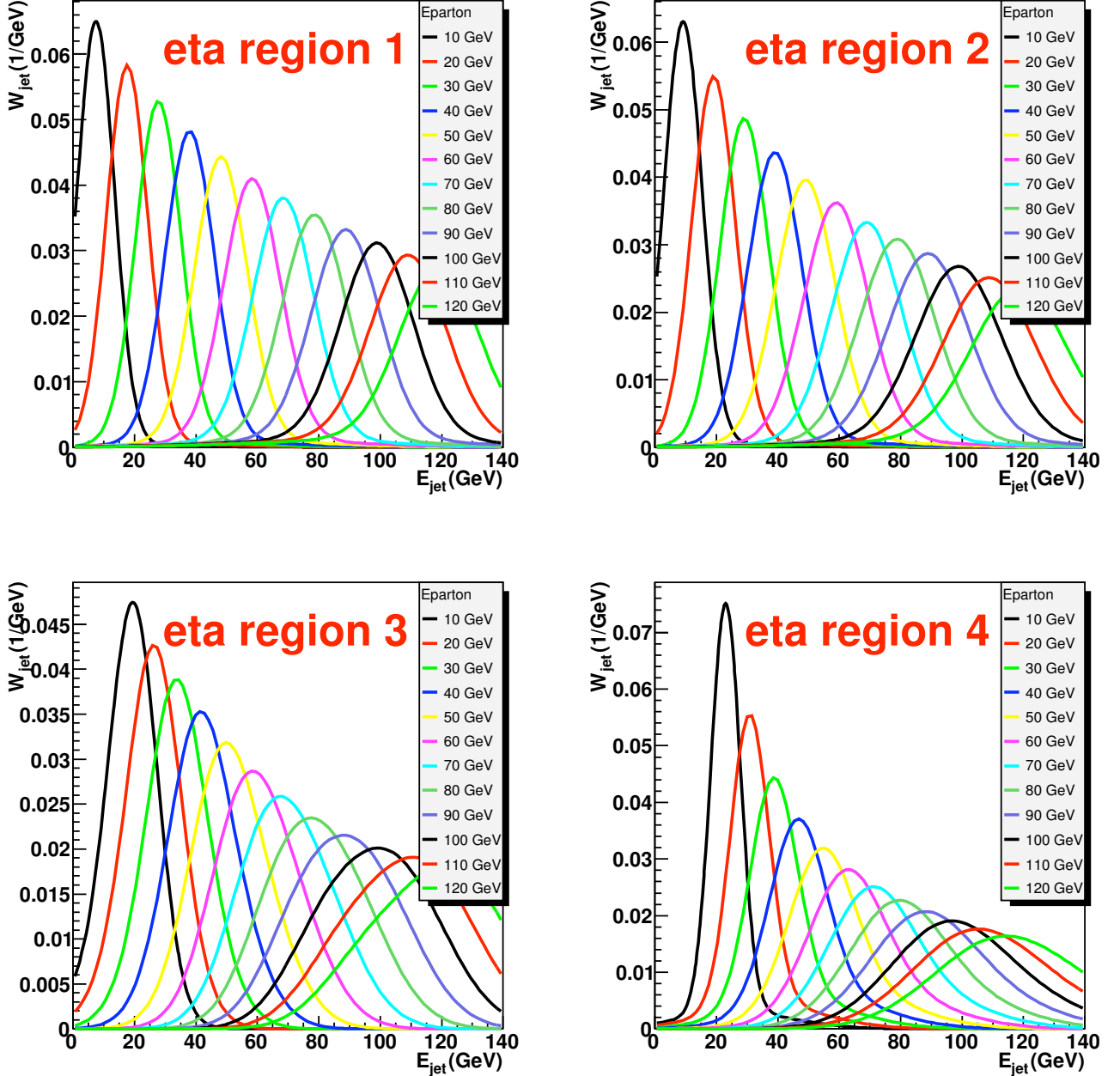


Figure 1: Transfer functions for light quark jets for different parton energies for the reference jet energy scale  $JES=1.00$  and for the following detector regions: (1)  $|\eta| < 0.5$ , (2)  $0.5 \leq \eta < 1.0$ , (3)  $1.0 \leq \eta < 1.5$ , and (4)  $1.5 \leq \eta$ . The  $x$ -axis  $E_{\text{jet}}$  in the plots ( $E_{\text{parton}}$  in the legends) corresponds to  $E_x$  ( $E_y$ ) in Eq. 4, while the  $y$ -axis corresponds to  $W_{\text{jet}}$  in Eq. 4.

The expression for the background probability  $P_{\text{bkg}}$  is similar to that for  $P_{\text{sig}}$  given in Eq. 2 except that the VECBOS [9] parameterization of the matrix element  $\mathcal{M}$  is used and all jets are assumed to be light. Since the matrix element for  $W$ +jets production does not depend on  $m_{\text{top}}$ ,  $P_{\text{bkg}}$  is independent of  $m_{\text{top}}$ .

In order to extract the top quark mass from a set of  $n$  measured events  $x_1, \dots, x_n$ , a likelihood function is built from the individual event probabilities calculated according to Eq. 1 as

$$L(x_1, \dots, x_n; m_{\text{top}}, JES, f_{\text{top}}) = \prod_{i=1}^n P_{\text{evt}}(x_i; m_{\text{top}}, JES, f_{\text{top}}). \quad (7)$$

For every assumed pair of values ( $m_{\text{top}}$ ,  $JES$ ), the value of  $f_{\text{top}}^{\text{best}}$  that maximizes the likelihood is determined. To obtain the best estimates of  $m_{\text{top}}$  and  $JES$ , the 2D likelihood:

$$L(x_1, \dots, x_n; m_{\text{top}}, JES) = L(x_1, \dots, x_n; m_{\text{top}}, JES, f_{\text{top}}^{\text{best}}(m_{\text{top}}, JES)) \quad (8)$$

is projected onto the  $m_{\text{top}}$  and  $JES$  axes:

$$L(x_1, \dots, x_n; m_{\text{top}}) = \int L(x_1, \dots, x_n; m_{\text{top}}, JES) G(JES^*) d(JES), \quad (9)$$

$$L(x_1, \dots, x_n; JES) = \int L(x_1, \dots, x_n; m_{\text{top}}, JES) d(m_{\text{top}}). \quad (10)$$

The prior  $G(JES^*)$  is a Gaussian function centered at  $JES^* = 1$  with width  $\sigma = 0.02$ , which corresponds to the relative uncertainty of the standard jet energy scale calibration determined from the photon+jets and dijet samples. Here  $JES^* = (JES + 0.007)/1.06$  is calibrated by using the curve shown in the left panel in figure 5 (see section IV). The mean and RMS of  $L(x_1, \dots, x_n; m_{\text{top}})$  and  $L(x_1, \dots, x_n; JES)$  are then used to extract the best estimate and the uncertainty of the top quark mass and those of  $JES$ , respectively.

## IV. CALIBRATION OF THE METHOD

### A. Ensemble Testing Procedure

The method of ensemble testing is used to calibrate the matrix element method, correcting for biases to ensure that the fitted parameters represent true values and that the estimated errors can be trusted. Each pseudo-experiment in an ensemble is formed by randomly drawing  $N_{\text{sig}}$  top quark pair signal and  $N_{\text{bkg}}$   $W$ +jets background events from a large pool of fully simulated MC events. These MC events are generated by ALPGEN, with PYTHIA simulating parton showers and hadronization. The  $D\emptyset$  detector responses are simulated by GEANT3. The size of each pseudo-experiment,  $N = N_{\text{sig}} + N_{\text{bkg}}$ , is fixed to the total number of events in the data sample while the relative proportions of signal and background events are allowed to fluctuate around a value determined from data (see section IV B). This procedure is repeated 1000 times.

### B. Determining the Signal Fraction from Data

The signal fractions before  $b$ -tagging are determined separately for the  $e$ +jets and  $\mu$ +jets channels. The relation of fitted versus true signal fraction is determined by repeating the ensemble testing procedure described in the previous section a number of times using a different value of the true signal fraction each time. In Fig. 2, we plot the mean of the fitted signal fractions from each ensemble test as a function of the true signal fraction separately for  $e$ +jets and  $\mu$ +jets channels. The relation is parameterized by a straight line. Using these fits, the calibrated signal fractions listed in Table I are extracted from the data.

| Channel     | Fitted Signal Fraction | Calibrated Signal Fraction |
|-------------|------------------------|----------------------------|
| $e$ +jets   | $0.268 \pm 0.042$      | $0.348 \pm 0.055$          |
| $\mu$ +jets | $0.333 \pm 0.047$      | $0.406 \pm 0.057$          |

Table I: Signal fractions determined from the data.

### C. Results of Ensemble Tests

The signal fractions determined from the previous section are used to compose each pseudo-experiment in the ensemble testing procedure described in section IV A. After drawing the signal and background events from the pool according to these fractions, we calculate the likelihoods for events with at least one  $b$ -tagged jet. Ensemble tests are performed on five different top quark pair production MC samples generated with top quark masses of  $m_{\text{top}}^{\text{gen}} = 165, 170, 172.5, 175, \text{ and } 180$  GeV with default jet energy scale corrections applied to the jets in each event ( $JES^{\text{gen}} = 1.00$ ). The same  $W$ +jets background sample (also at  $JES^{\text{gen}} = 1.00$ ) is used in each case. Two additional  $JES$  shifted samples

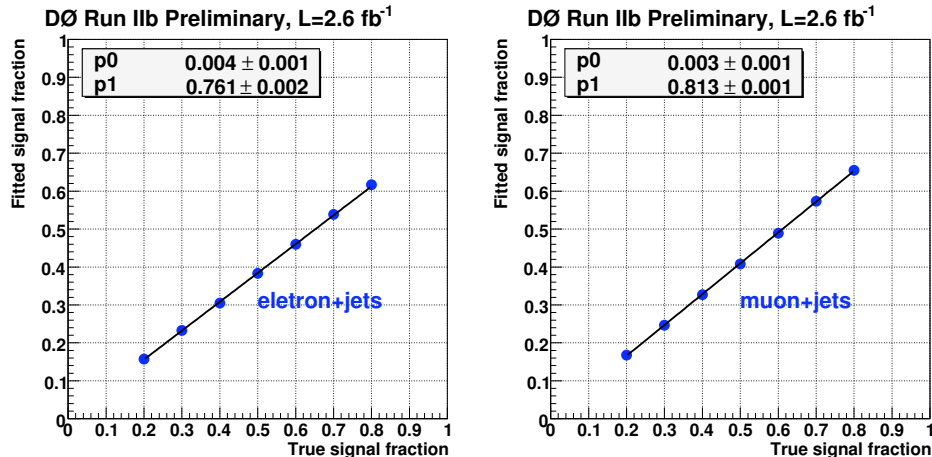


Figure 2: Fitted signal fraction as a function of true signal fraction for  $e$ +jets (left) and  $\mu$ +jets (right) channels.

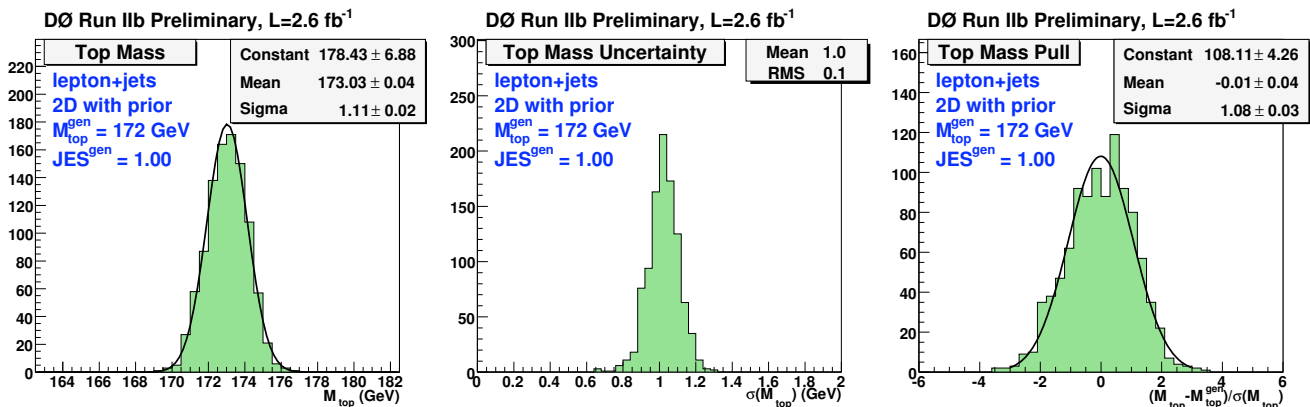


Figure 3: Distributions of fitted top quark masses, uncertainties, and pulls from ensemble tests performed on  $M_{\text{top}}^{\text{gen}} = 172.5$  GeV and  $JES^{\text{gen}} = 1.00$  MC samples.

are produced from the  $M_{\text{top}}^{\text{gen}} = 172.5$  GeV top pair production MC sample where all jet energies are scaled up by 5% ( $JES^{\text{gen}} = 1.05$ ) in one case and down by 5% ( $JES^{\text{gen}} = 0.95$ ) in the other. Two such samples are also produced for the  $W$ +jets background to be used with the corresponding top pair production sample.

For each ensemble test, a best estimate of  $m_{\text{top}}$  is determined for each pseudo-experiment from the mean of the projection of the 2D likelihood distribution onto the  $m_{\text{top}}$  axis (see Eq. 9). The distributions of the fitted top quark masses, uncertainties, and pulls [10] obtained from the ensemble tests performed with  $M_{\text{top}}^{\text{gen}} = 172.5$  GeV and  $JES^{\text{gen}} = 1.00$  are shown in Fig. 3. The means of the fitted top quark masses and their pull widths from each ensemble test are plotted as a function of the true top quark mass in Fig. 4. They are then fitted to straight lines which are used later in calibrating the data results. Similarly, the extracted  $JES$  and pull widths as a function of the true  $JES$  value are fitted to straight lines in Fig. 5.

## V. SYSTEMATIC UNCERTAINTIES

### A. Physics Modeling

#### 1. Higher Order Effects

The top quark pair MC samples used in the above ensembles tests are generated using the leading order generator ALPGEN. In order to study the influence of next-to-leading order QCD corrections, we compare a top quark pair MC sample generated by MC@NLO with a sample generated by ALPGEN. In order to avoid double-counting any other

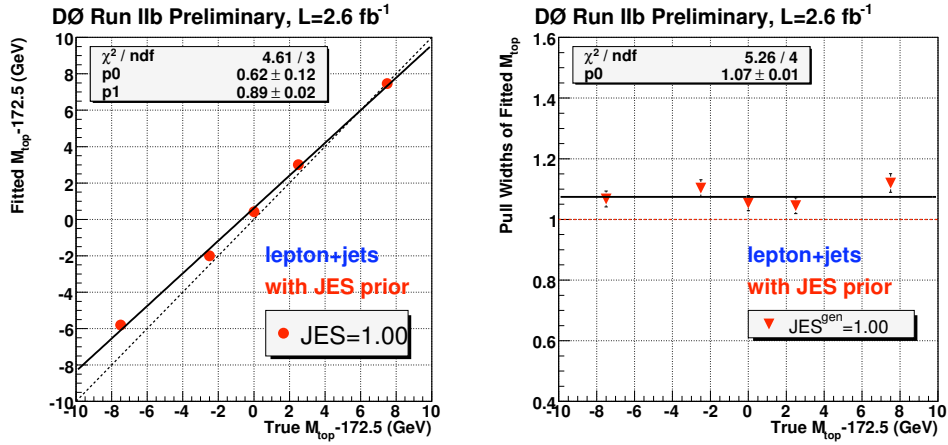


Figure 4: Fitted  $m_{\text{top}}$  and pull widths as a function of true  $m_{\text{top}}$  with  $JES^{\text{gen}}=1.00$ .

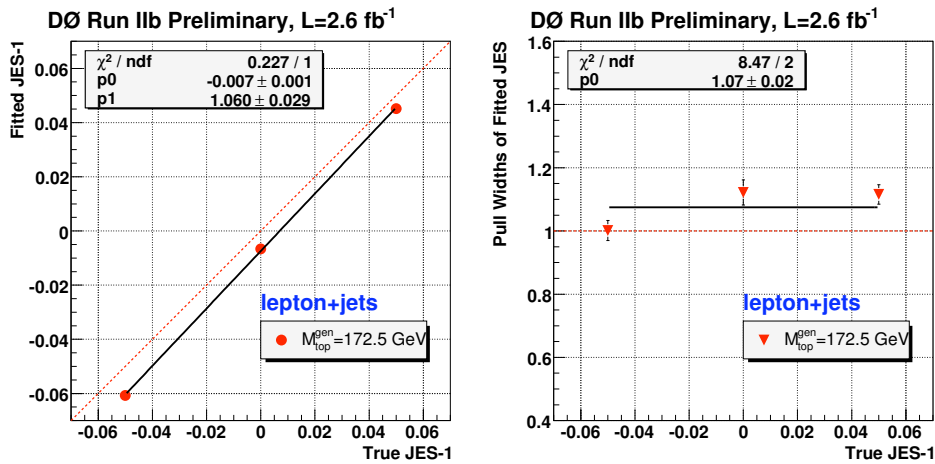


Figure 5: Fitted  $JES$  and pull widths as a function of true  $JES$  with  $M_{\text{top}}^{\text{gen}} = 172.5$  GeV.

effect, both samples use HERWIG to simulate parton showers and hadronization. We take the difference in the fitted top quark mass between these two samples as a systematic uncertainty.

## 2. ISR/FSR

The main contribution from this source comes from uncertainties in the modeling of extra jets due to initial state radiation or final state radiation (ISR/FSR). To evaluate this contribution we run on PYTHIA samples in which the amount of ISR and FSR has been increased and decreased according to Drell-Yan data by the CDF collaboration [11]. We take half the difference between the increased and decreased samples as our uncertainty.

## 3. Hadronization and Underlying Event

We compare two ALPGEN top quark pair samples which use respectively PYTHIA and HERWIG to model parton showers and hadronization, as well as underlying events. We assign the difference in the fitted top quark mass between the two samples as a systematic uncertainty.

#### 4. Color Reconnection

Various PYTHIA tunes using different models of color reconnection are investigated. These effects on the top mass measurement from a MC-truth level study are found to be about 0.5 GeV [12]. A preliminary estimate of these effects performed by CDF with a full mass reconstruction finds a difference of 0.40 GeV between two PYTHIA 6.4 tunes with and without color reconnection enabled [13]. For this preliminary result, we assign a 0.40 GeV uncertainty for the color reconnection effects.

#### 5. Multiple Hadron Interaction

Zero-bias events taken at different luminosities are overlaid onto the MC samples to simulate multiple interactions per beam crossing. We assign the change in the fitted top quark mass as a systematic uncertainty when the MC samples are reweighted to have different instantaneous luminosity distributions.

#### 6. Background Modeling

To evaluate this systematic, we identify distributions with poor agreement between data and MC in the background-dominated samples. Ensemble tests are then performed with all the background samples reweighted to match the distributions in data. The difference in the fitted top quark mass between the ensemble tests with the reweighted background events and that with the default background events is then taken as a systematic uncertainty.

#### 7. $W$ +Jets Heavy Flavor Factor

When  $b$ -tagging is applied, MC and data samples are known to disagree on the magnitude of the  $W$ +heavy flavor (HF) jets contribution to the  $W$ +jets background. A HF factor is introduced to the weights of the  $W$ +HF jets MC samples to increase their relative contributions in the  $W$ +jets background. Ensemble tests are repeated when MC sample compositions are determined with the HF factor varied from its central value by its uncertainty. The change in the fitted top mass is taken as a systematic uncertainty.

#### 8. $b$ -Modeling

We study possible effects in modeling of  $b$ -fragmentation. Alternative models for the fragmentation of  $b$ -quarks are implemented in the simulation by reweighting MC events [15]. These events are used to rederive the calibration curve. The default MC samples used in this analysis consist of events that have been reweighted from the default PYTHIA  $b$ -fragmentation function to a Bowler scheme [14] that has been tuned to LEP (ALEPH, OPAL, and DELPHI) data. To evaluate the systematics, these events were further reweighted to account for differences in SLD and LEP data.

The reconstructed energy of  $b$ -jets containing a semileptonic bottom or charm decay is in general lower than that of jets containing only hadronic decays. This can only be taken into account for jets in which a soft muon is reconstructed. Thus, the fitted top quark mass still depends on the semileptonic  $b$  and  $c$  decay branching ratios. A separate systematic uncertainty is assigned to take into account this effect.

#### 9. PDF Uncertainty

To evaluate this systematic, the default  $M_{\text{top}}^{\text{gen}}=172.5$  GeV MC signal sample generated by PYTHIA is reweighted to match each of the  $2 \times 20$  error parton distribution functions (PDFs) provided for CTEQ6M [16]. Ensemble tests are repeated for each of these variations and the uncertainty evaluated following the recommended procedure of [16].



## B. Detector Modeling

### 1. Residual JES Uncertainty

The relative difference between the jet energy scales in data and MC simulation has been fitted with the global scale factor  $JES$ , and the corresponding uncertainty is included in the quoted (stat+JES) uncertainty. However, the difference between the jet energy scales in data and MC simulation may not be just a global scale difference, and thus may lead to an additional uncertainty on the top quark mass. To estimate this uncertainty, the energy of each jet in a top quark pair MC sample is scaled by a factor parameterized as a function of  $p_T$  and  $\eta$ . This parameterization corresponds to the quadratic sum of the uncertainties of the jet energy scale in data and MC. The parameterization is shifted down in such a way that the average scale shift applied to all jets is zero. Probabilities are recalculated for the scaled sample and the resulting change in the fitted top quark mass with respect to the unscaled one is taken as the systematic uncertainty.

### 2. Relative $b$ /Light Jet Energy Scale

There are differences in the  $b$ /light jet energy scale ratio between data and simulation. To estimate this difference, jets are constructed at the particle level in the top quark pair MC sample for each event classifying them as  $b$ -jets or light jets. Single particle response curves for both data and MC samples are then applied to the particle jets to predict what the energy of a reconstructed jet in the calorimeter would be. From these reconstructed energies, the ratio  $p_T^{\text{data}}/p_T^{\text{MC}}$  is then calculated separately for both  $b$ -jets and light jets and the double ratio evaluated:

$$\frac{(p_T^{\text{data}}/p_T^{\text{MC}})_{b\text{-jet}}}{(p_T^{\text{data}}/p_T^{\text{MC}})_{\text{light jet}}} \quad (11)$$

resulting in a difference of 1.8%. Using this result, all jets that could be matched to a  $b$ -parton in the  $m_{\text{top}}^{\text{gen}} = 172.5$  GeV MC sample used in the calibration are scaled by this amount. Ensemble tests are repeated with the scaled sample and the difference in the fitted top quark mass with the default sample is taken as the systematic uncertainty.

### 3. Sample-Dependent Jet Energy Scale

The jet energy scale corrections in MC are shifted to take into account the difference with respect to data. The shifting is different for quark jets and for gluon jets. A systematic uncertainty is introduced to take into account this sample-dependent jet energy scale. It is given by the change in the extracted top mass from MC when the jet energy scale shifting is turned on or off in MC samples.

### 4. $b$ -Tagging Efficiency

Ensemble tests are repeated to study the effects from the uncertainty in the  $b$ -tagging efficiency. The tag rate functions for the  $b$ -quark and  $c$ -quark and the mistag rate function for the light quarks are varied within their uncertainties. The difference in the fitted top mass is taken as a systematic uncertainty.

### 5. Trigger Efficiency

Events in MC samples have been reweighted according to the trigger efficiencies measured in data. To evaluate the effects due to trigger efficiency uncertainty, we simply remove the trigger weights (i.e. set them to unity) and then rederive the calibration and apply this to the data result. The difference from that obtained with the trigger weights is taken as a systematic uncertainty.

### 6. Lepton Momentum Scale

There is a difference in the lepton momentum scale between MC and data. Such a difference is corrected for in a MC sample and the change in the fitted top mass is assigned as a systematic uncertainty.

### 7. Jet Energy Resolution

The jet energy resolution in the MC simulation has been tuned in order to match the jet energy resolution measured in data. To evaluate the effects due to the jet energy resolution uncertainty, an ensemble test is done on MC samples in which the jet energy resolution is varied within its uncertainty. Half of the difference from that obtained with the default jet energy resolution is taken as a systematic uncertainty.

### 8. Jet Identification Efficiency

There is some uncertainty associated with the scale factors used to achieve data/MC agreement in jet Identification efficiencies. To evaluate the effect of this source on the top quark mass, the jet identification efficiencies in the  $m_{\text{top}}^{\text{gen}} = 172.5$  GeV signal sample are varied according to these uncertainties. We use the number evaluated in the previous analysis [6] for this preliminary result.

## C. Method

### 1. Multijet Background

The  $W$ +jets simulation is used to model the small multijet background in the selected event sample in the analysis. The systematic uncertainty from this assumption is computed by selecting a dedicated multijet-enriched sample of events from data by inverting the lepton isolation cut in the event selection. The ensemble test done at  $m_{\text{top}}^{\text{gen}} = 172.5$  GeV in the calibration of the method is repeated with this multijet-enriched sample included in the composition. The difference in the fitted top quark mass when this background sample is included is taken as the systematic uncertainty.

### 2. Signal Fraction

The signal fractions determined from data and used in the ensemble tests are associated with statistical uncertainties. These signal fractions are varied by their uncertainties independently for each decay channel and the ensemble tests are repeated for all MC samples to rederive the mass calibration curves. The resulting uncertainties in the top quark mass in each decay channel are then added in quadrature, half of which is assigned as a systematic uncertainty.

### 3. MC Calibration

This systematic uncertainty is estimated by varying the calibration of the top mass measurement according to the statistical uncertainty of the linear fit shown in Fig. 4.

## D. Summary of Systematic Uncertainties

The systematic uncertainties for the Run IIb  $b$ -tagged analysis described in this note are summarized in Table II. The systematic uncertainties for the Run IIa  $b$ -tagged analysis [6] are also summarized in Table II. Note that the systematic uncertainties for higher order effects, hadronization and underlying event, color reconnection, the lepton momentum scale, as well as sample-dependent JES, which were not considered in Ref. [6], are added with the numbers taken from the Run IIb analysis.

## VI. RESULTS

The results from the  $2.6 \text{ fb}^{-1}$  of Run IIb data after the calibration are shown in Figs. 6, 7, and 8. The statistical+ $JES$  uncertainty for the top quark mass has been inflated by the averaged pull width shown in Fig. 4, and has been determined to be 1.28 GeV. As shown in the right panel of Fig. 7, the expected value of this uncertainty is found to be 1.22 GeV from the ensemble tests. The statistical+ $m_{\text{top}}$  uncertainty for  $JES$  is determined to be

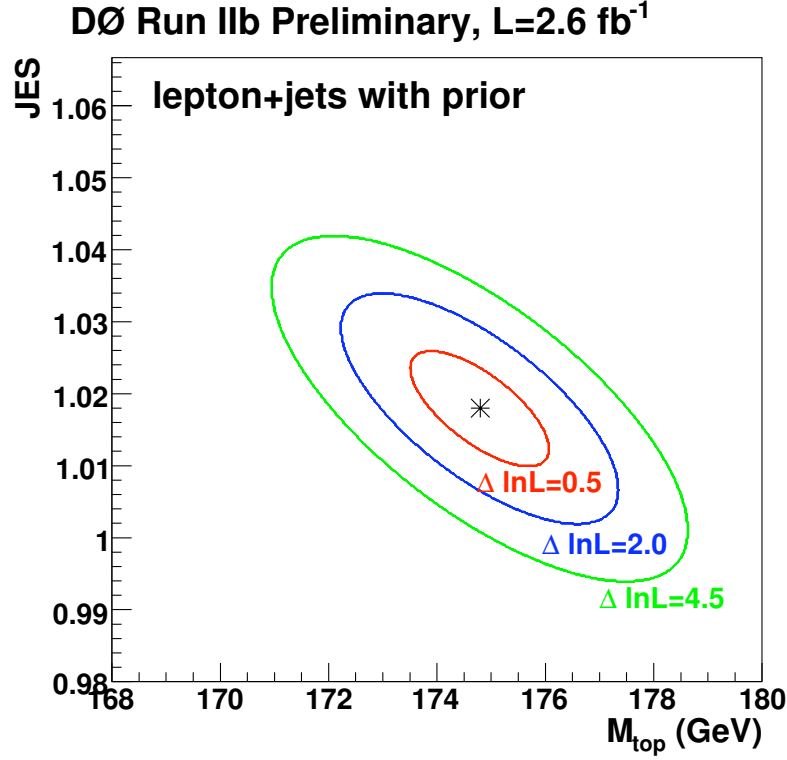


Figure 6: Calibrated results of the 2D analysis on Run IIb data.

| Source                            | Uncertainty on top mass in Run IIb (GeV) | Uncertainty on top mass in Run IIa (GeV) |
|-----------------------------------|--|--|
| Higher Order Effects              | ±0.25                                    | ±0.25                                    |
| ISR/FSR                           | ±0.26                                    | ±0.40                                    |
| Hadronization and UE              | ±0.58                                    | ±0.58                                    |
| Color Reconnection                | ±0.40                                    | ±0.40                                    |
| Multiple Hadron Interactions      | ±0.07                                    | ±0.01                                    |
| Background Modeling               | ±0.03                                    | ±0.04                                    |
| W HF factor                       | ±0.07                                    | ±0.09                                    |
| <i>b</i> -Modeling                | ±0.09                                    | ±0.03                                    |
| PDF Uncertainty                   | ±0.24                                    | ±0.14                                    |
| Residual JES Uncertainty          | ±0.21                                    | ±0.10                                    |
| Relative <i>b</i> /Light Response | ±0.81                                    | ±0.83                                    |
| Sample-Dependent JES              | ±0.56                                    | ±0.56                                    |
| <i>b</i> -Tagging Efficiency      | ±0.08                                    | ±0.15                                    |
| Trigger Efficiency                | ±0.01                                    | ±0.19                                    |
| Lepton Momentum Scale             | ±0.17                                    | ±0.17                                    |
| Jet Identification Efficiency     | ±0.26                                    | ±0.26                                    |
| Jet Energy Resolution             | ±0.32                                    | ±0.03                                    |
| QCD Background                    | ±0.14                                    | ±0.14                                    |
| Signal Fraction                   | ±0.10                                    | ±0.09                                    |
| Muon Resolution                   | -  | ±0.10                                    |
| Signal Contamination              | -  | ±0.13                                    |
| MC Calibration                    | ±0.20                                    | ±0.26                                    |
| Total                             | ±1.41                                    | ±1.43                                    |

Table II: Systematic uncertainties for the Run IIb and Run IIa *b*-tagged analyses. The systematic uncertainties for higher order effects, hadronization and underlying event, color reconnection, lepton momentum scale, as well as sample-dependent JES, which were not considered in Ref. [6], are added for the Run IIa analysis with the numbers taken from the Run IIb analysis.

0.008; this has been inflated by the averaged pull width shown in Fig. 5. As shown in the right panel of Fig. 8, the expected value of this uncertainty is found to be 0.008 from the ensemble tests. The final result for the top quark

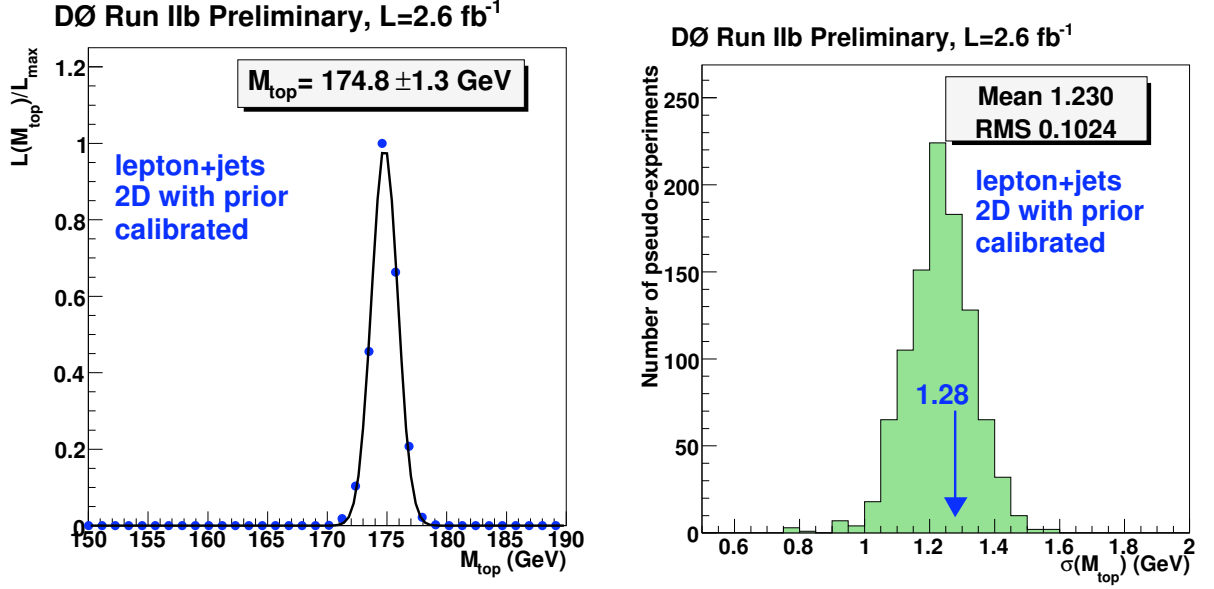


Figure 7: Calibrated top mass results of the 2D analysis on Run IIb data. The plot in the left panel is a projection of  $L(m_{\text{top}}, JES)$  onto the  $m_{\text{top}}$  axis. The uncertainty in the left plot has been inflated by the average pull width of  $m_{\text{top}}$  from Fig. 4. This inflated uncertainty is indicated by the vertical arrow in the distribution in the right plot showing distributions of  $\sigma(m_{\text{top}})$  from the ensemble test performed at  $m_{\text{top}}^{\text{gen}} = 172.5 \text{ GeV}$  and  $JES^{\text{gen}} = 1.00$ .

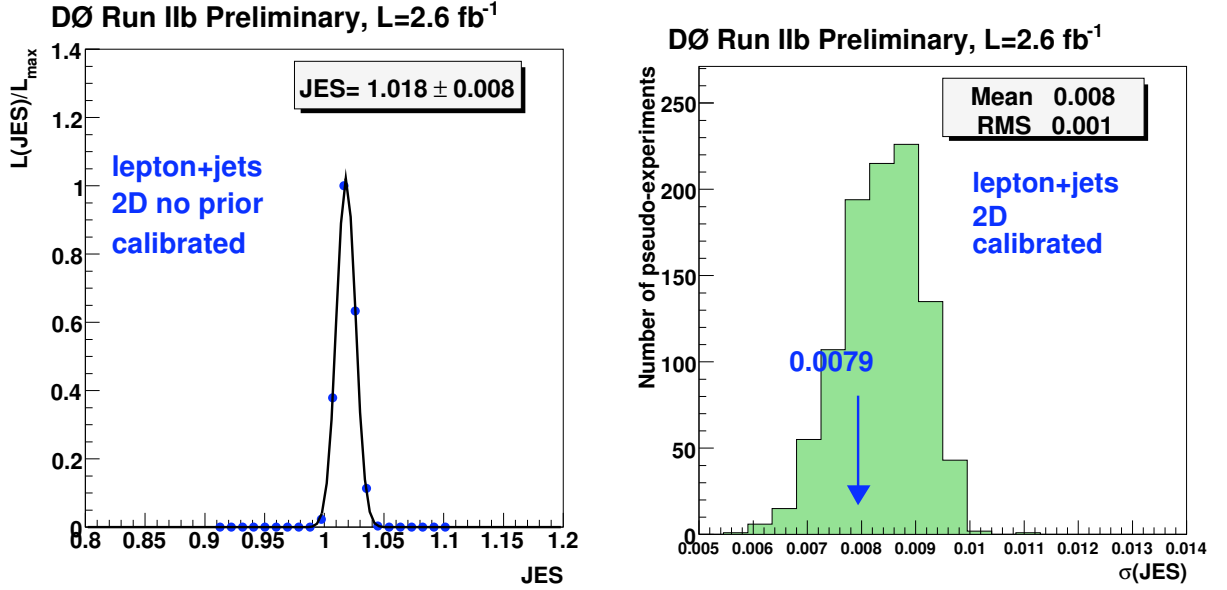


Figure 8: Calibrated  $JES$  of the 2D analysis on Run IIb data. The plot in the left panel is a projection of  $L(m_{\text{top}}, JES)$  onto the  $JES$  axis. The uncertainty in the left plot has been inflated by the average pull width of  $JES$  from Fig. 5. This inflated uncertainty is indicated by the vertical arrow in the distribution in the right plot showing distributions of  $\sigma(JES)$  from the ensemble test performed at  $m_{\text{top}}^{\text{gen}} = 172.5 \text{ GeV}$  and  $JES^{\text{gen}} = 1.00$ .

mass, together with the systematic uncertainty from the previous section is:

$$m_{\text{top}} = 174.75 \pm 1.28(\text{stat} + JES) \pm 1.41(\text{sys}) \text{ GeV}. \quad (12)$$

The final result for  $JES$  is

$$JES = 1.018 \pm 0.008(\text{stat} + m_{\text{top}}). \quad (13)$$

This number is consistent with the standard jet energy calibration derived from photon+jets and dijet samples; the latter has a relative uncertainty of about 2%.

The result for the top quark mass from the  $b$ -tagged analysis on  $1.0 \text{ fb}^{-1}$  of Run IIa data is [6] (see also table II):

$$m_{\text{top}} = 171.46 \pm 1.76(\text{stat} + \text{JES}) \pm 1.43(\text{syst}) \text{ GeV}. \quad (14)$$

Combining the two top quark mass results using the BLUE method [17, 18], the top quark mass for the full  $3.6 \text{ fb}^{-1}$  of Run II data set is

$$m_{\text{top}} = 173.748 \pm 0.83(\text{stat}) \pm 1.62(\text{syst}) = 173.7 \pm 1.8 \text{ GeV}. \quad (15)$$

Here the uncertainty from  $JES$  on the top quark mass is included in the systematic uncertainty in the combined result, while it is included in the “stat+JES” uncertainty in the individual results. The combination uses the same uncertainty classes and method as used by the Tevatron Electroweak Working Group in their top mass combinations [19]. The combination yields a  $\chi^2$  of 2.53 for 1 degree of freedom, which corresponds to a probability of 11.2%.

### Acknowledgments

We thank the staffs at Fermilab and collaborating institutions, and acknowledge support from the DOE and NSF (USA); CEA and CNRS/IN2P3 (France); FASI, Rosatom and RFBR (Russia); CNPq, FAPERJ, FAPESP and FUNDUNESP (Brazil); DAE and DST (India); Colciencias (Colombia); CONACyT (Mexico); KRF and KOSEF (Korea); CONICET and UBACyT (Argentina); FOM (The Netherlands); STFC (United Kingdom); MSMT and GACR (Czech Republic); CRC Program, CFI, NSERC and WestGrid Project (Canada); BMBF and DFG (Germany); SFI (Ireland); The Swedish Research Council (Sweden); CAS and CNSF (China); and the Alexander von Humboldt Foundation.

- 
- [1] F. Abe *et al.* (CDF Collaboration), Phys. Rev. Lett. **74**, 2626 (1995).
  - [2] S. Abachi *et al.* (DØ Collaboration), Phys. Rev. Lett. **74**, 2632 (1995).
  - [3] V.M. Abazov *et al.* (DØ Collaboration), Nature **429**, 638 (2004).
  - [4] V.M. Abazov *et al.* (DØ Collaboration), Phys. Rev. D **74**, 092005 (2006).
  - [5] V.M. Abazov *et al.* (DØ Collaboration), Phys. Rev. D **75**, 092001 (2007).
  - [6] V.M. Abazov *et al.* (DØ Collaboration), Phys. Rev. Lett. **101**, 182001 (2008).
  - [7] V.M. Abazov *et al.* (DØ Collaboration), DØ Note 5750-CONF (2008).
  - [8] V.M. Abazov *et al.* (DØ Collaboration), Nucl. Instrum. Methods A **565**, 463 (2006).
  - [9] F.A. Berends *et al.*, Nucl. Phys. B **357**, 32 (1991).
  - [10] The pull is the difference between the fitted and true top masses divided by the fitted uncertainty of the top mass.
  - [11] CDF note 6804 (2004), [http://hep.uchicago.edu/~hslee/ISR/cdf6804\\_ISR\\_DY.ps](http://hep.uchicago.edu/~hslee/ISR/cdf6804_ISR_DY.ps)
  - [12] D. Wicke and P. Skands, arXiv:0807.3248 [hep-ph] (2008).
  - [13] CDF public note 9692 (2009).
  - [14] M.G. Bowler, Z. Phys. C **11**, 169 (1981).
  - [15] Y. Peters, K. Hamacher and D. Wicke, FERMILAB-TM-2425-E (2009).
  - [16] J. Pumplin *et al.*, J. High Energy Phys. **0207**, 012 (2002).
  - [17] L. Lyons, D. Gibaut, and P. Clifford, Nucl. Instrum. Meth. A **270**, 110 (1988).
  - [18] A. Valassi, Nucl. Instrum. Meth. A **500**, 391 (2003).
  - [19] The Tevatron Electroweak Working Group for the CDF and DØ collaborations, arXiv:0808.1089 [hep-ex] (2008).